Journal of Earth Science, *Vol. 25*, *No. 3*, *p. 460–472*, *June 2014* *ISSN 1674-487X*
Printed in China
DOI: 10.1007/s12583-014-0449-z

Geochemistry of Rare Earth Elements (REE) in the Weathered Crusts from the Granitic Rocks in Sulawesi Island, Indonesia

Adi Maulana*[1], Kotaro Yonezu[2], Koichiro Watanabe[2]
1. *Department of Geology Engineering*, *Faculty of Engineering*, *Hasanuddin University*, 90245 *Makassar*, *Indonesia*
2. *Department of Earth Resources Engineering*, *Kyushu University*, *Fukuoka* 8190395, *Japan*

ABSTRACT: We report for the first time the geochemistry of rare earth elements (REE) in the weathered crusts of I-type and calc-alkaline to high-K (shoshonitic) granitic rocks at Mamasa and Palu region, Sulawesi Island, Indonesia. The weathered crusts can be divided into horizon A (lateritic profile) and B (weathered horizon). Quartz, albite, kaolinite, halloysite and montmorrilonite prevail in the weathered crust. Both weathered profiles show that the total REE increased from the parent rocks to the horizon B but significantly decrease toward the upper part (horizon A). LREE are enriched toward the upper part of the profile as shown by La/Yb_N value. However, HREE concentrations are high in horizon B1 in Palu profile. The total REE content of the weathered crust are relatively elevated compared to the parent rocks, particularly in the lower part of horizon B in Mamasa profile and in horizon B2 in Palu profile. This suggests that REE-bearing accessory minerals may be resistant against weathering and may remain as residual phase in the weathered crusts. The normalized isocon diagram shows that the mass balance of major and REE components between each horizon in Mamasa and Palu weathering profile are different. The positive Ce anomaly in the horizon A of Mamasa profile indicated that Ce is rapidly precipitated during weathering and retain at the upper soil horizon.
KEY WORDS: rare earth element, geochemistry, weathered crust, granitic rock, Sulawesi, Indonesia.

1 INTRODUCTION

Rare earth elements (REE) are defined as members of Group IIIA in the periodic table which consist of lanthanum to luthetium (^{57}La to ^{71}Lu), including Yttrium (^{39}Y) and Scandium (^{21}Sc) (Henderson, 1984). They can be divided into light rare earth elements (La to Eu) and heavy rare earth elements (Gd to Lu) which commonly abbreviated as LREE and HREE, respectively. For many years, rare earth elements have been geochemically considered immobile during alteration and metamorphism and therefore very useful in geological interpretation (Winchester and Floyd, 1976; Condie and Baragar, 1974; Pearce and Cann, 1973). Nevertheless, recent studies have shown that the abundance of REE is subjected to change during alteration and weathering process, particularly in the upper crust (Bao and Zhao, 2008; Nesbitt and Young, 1984; Gouveia et al., 1993; Braun et al., 1990; Henderson, 1984; Alderton et al., 1980). One of the most prominent studies on REE behavior during alteration and weathering in the upper crust is in granitic rocks since these rocks contain much abundant of REE compared to other crustal rocks (Hu and Gao, 2008).

The granitic rocks are widely distributed in Sulawesi Island in the central part of Indonesian Archipelago (Sukamto, 1975). They occupy the western part to the northern part of the island, encompassing for more than 400 km. The island is situated in the equatorial line and hence is located in tropical climate, causing the surface of the rocks is susceptible to weathering and alteration process. It has been reported that REE are mobile and tend to be enriched during weathering of granitic rocks in some subtropic areas (Bao and Zhao, 2008; Ishihara et al., 2008). In addition, enrichments of REE in weathered granitic crusts from tropic areas were also reported (Sanematsu et al., 2011, 2009). Therefore, investigation on REE enrichment on the granitic rocks in this island is of particular interest in order to shed a light on their geochemistry.

However, regardless their large distribution, study on geochemistry of REE in the weathered crust of granitic rocks in Sulawesi Island has never been conducted. This paper reports for the first time, the REE geochemistry in weathered crust of granitic rocks in Sulawesi Island, Indonesia, particularly from Mamasa and Palu regions.

2 REGIONAL GEOLOGY

The Mamasa and Palu regions are located in the western and central Sulawesi (Fig. 1), respectively. They are separated by mountainous topography consisting of Tertiary and Quaternary volcanic rocks.

The general geology of Mamasa region is shown in Fig. 1b, which consists of five sequences (Djuri and Sudjatmiko,

*Corresponding author: adi-maulana@unhas.ac.id

Manuscript received April 13, 2013.
Manuscript accepted August 18, 2013.

Maulana, A., Yonezu, K., Watanabe, K., 2014. Geochemistry of Rare Earth Elements (REE) in the Weathered Crusts from the Granitic Rocks in Sulawesi Island, Indonesia. *Journal of Earth Science*, 25(3): 460–472, doi:10.1007/s12583-014-0449-z

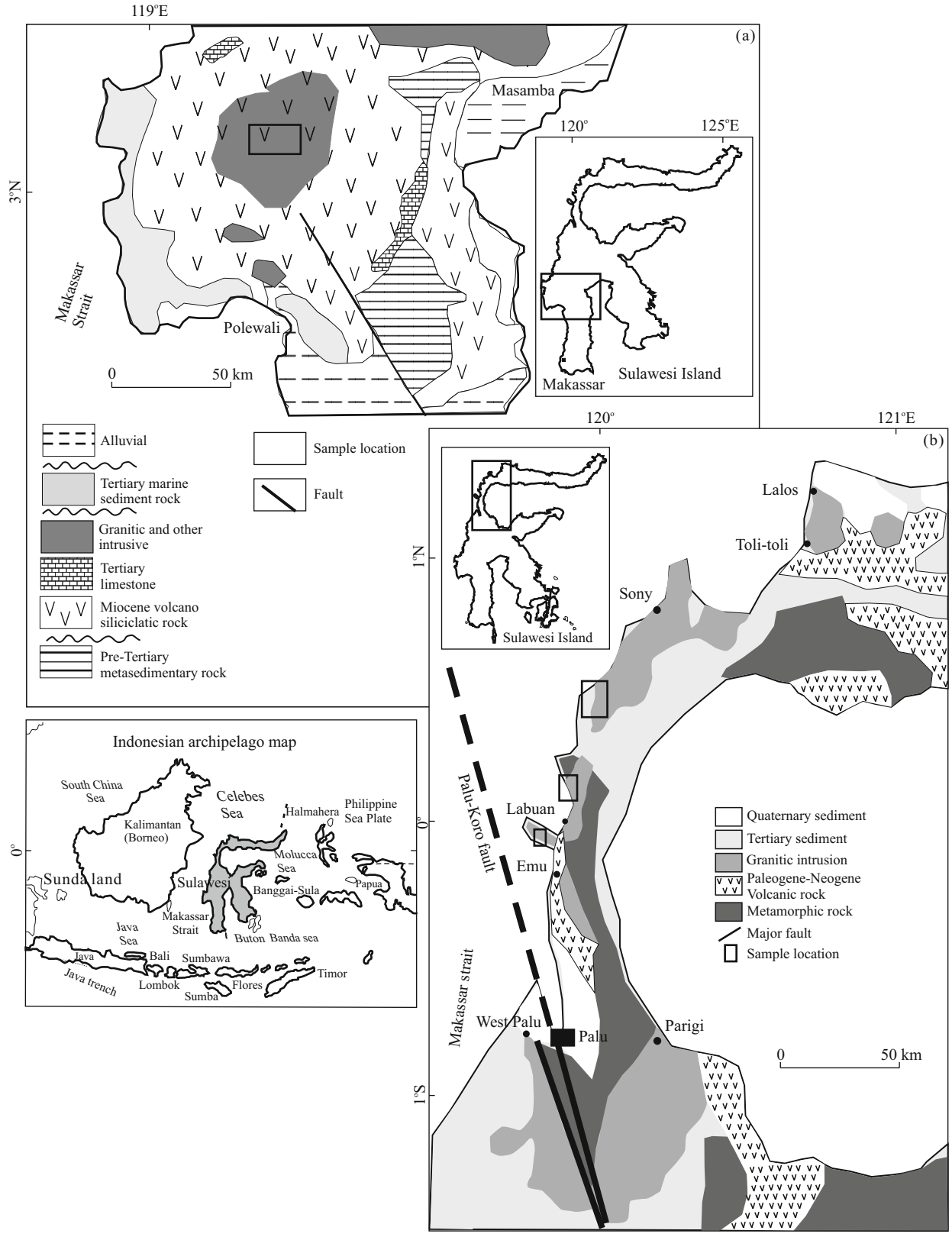

Figure 1. Geologic map and location of studied area of (a) Mamasa and (b) Palu.

1998): (1) Pre-Tertiary metasedimentary rocks including flysch deposits which were formed in a forearc basin setting, and ophiolites of Lamasi Complex; (2) Miocene to Pliocene syn-rifting sequence composed of siliciclastic, coal, volcanic and carbonates sedimentary deposit of the Toraja and Mallawa Formation; (3) Tertiary post-rifting sequence including the Eocene to Middle Miocene carbonate Makale and Tonasa limestone; (4) Middle Miocene to Pliocene granitic to gabbroic intrusive rocks (known as Mamasa granitic rocks); (5) Pliocene to recent non marine to upper bathyal sedimentary deposits

including Walanae Formation.

Palu region is included in the Central Sulawesi Terrane, located between Central Sulawesi metamorphic belt in the east and Lariang-Karama Basin in the south (Parkinson, 1998; Hamilton, 1979). The area is cross cut by regional fault structure, called Palu-Koro fault, trending from northwest to southeast (Fig. 1b). The regional geology consists of five units namely; (1) Pre-Tertiary metamorphic rocks, (2) Paleogen–Neogen volcanic rocks, (3) Miocene granitic intrusion, (4) Tertiary sediments and (5) Quaternary sediments.

Metamorphic rocks in this area are mainly assigned to the Palu metamorphic complex (Parkinson, 1998) in the central portion and Malino metamorphic complex in the north (Van Leeuwen et al., 2007). They consist of metabasic rocks metamorphosed to greenschist-amphibolite facies. The Paleogene–Neogen volcanic rocks are exposed in southern part and middle part of the terrane. They consist of andesitic tuff, lithic tuff and felsic crystal tuff as well as laminated sandstone (Sukamto, 1996). The granitic suites in this terrane consist of quartz monzonite to quartz dioritic rocks (Priadi et al., 1996). The Tertiary sediment includes large amount of mollase sediment, conglomerate, sandstone which are poorly consolidated. Quaternary sediments are exposed along the coastline of the terrane, consisting of alluvium, coastal deposit, gravel, sand, mud and coral reef (Sukamto, 1996).

3 DESCRIPTION OF THE PARENT ROCKS AND WEATHERING PROFILE

Due to intensive weathering process, the parent rocks are rarely exposed in the base of the weathering profile. Instead, they are mainly found in a lower topography such as in the river bank and the cliff of the hill. We choose the nearest fresh sample to the weathering profile within the same pluton body as the parent rocks.

3.1 Mamasa Granites

The Mamasa granitic rocks have been moderately to heavily weathered. They consist of granite, granodiorite, diorite and quartz monzonite (Maulana et al., 2011; Elburg and Foden, 1999). The petrography of the parent rocks reveals that mineralogy and textures of the granitic rocks are fairly uniform but different in ratio throughout all samples. The parent rock samples show equigranular texture, coarse to medium grained and sometimes show porphyritic texture with plagioclase occurs as phenocryst (Maulana et al., 2011). Quartz, plagioclase, K-feldspar, biotite and hornblende commonly occur with accessory mineral of titanite, apatite, zircon, allanite, magnetite and ilmenite whereas chlorite occurs as secondary minerals. Some enclaves have mafic composition. K-Ar dating on whole rock of quartz monzodiorite yielded a range from 7.7±0.2 to 7.0±0.3 Ma (Bergman et al., 1996) whereas an age range from 14.1±0.1 to 4.6±0.3 Ma on K-feldspar and biotite were reported in quartz diorite from Mamasa intrusive rocks (Elburg et al., 2003). Most of the granitic rocks are classified as high calc-alkaline (CAK) to high-K or shoshonitic group. Based on the alumina saturation index (ASI) the granitic rocks belong to I-type granitic rocks (ASI ranges from 0.95 to 1.0) (Maulana et al., 2011).

The weathered crusts in Mamasa range from 1 to 4 m in thickness (Fig. 2a). Overall, weathered crusts show brown to yellowish color, are highly oxidized and poorly compacted, enriched in clay minerals. Rock forming minerals were decomposed except quartz as shown in XRD results. One section (ML-50) of the weathered crusts in Mamasa shows weathering profile and can be divided into horizon A (lateritic profile) and horizon B (weathered horizon) (Fig. 2). The horizon A belongs to the upper part of the profile (from 0 to 0.7 m depth), which is characterized by dark brown in color, abundant organic matter and poorly compacted. The horizon B is found in the lower part of the section (from 0.7–3.4 m depth), reddish brown in color and composed mainly of clay minerals and lesser amount of organic matters.

3.2 Palu Granites

The Palu granitic rocks range from monzonite to granodiorite with gabbroic enclaves (Maulana et al., 2011). Quartz, plagioclase and alkali feldspar found as major minerals and sometimes occur as phenocrysts. Quartz is medium to coarse grained showing undulose extinction. Plagioclase is tabular, ranges from oligoclase to labradorite, showing typical

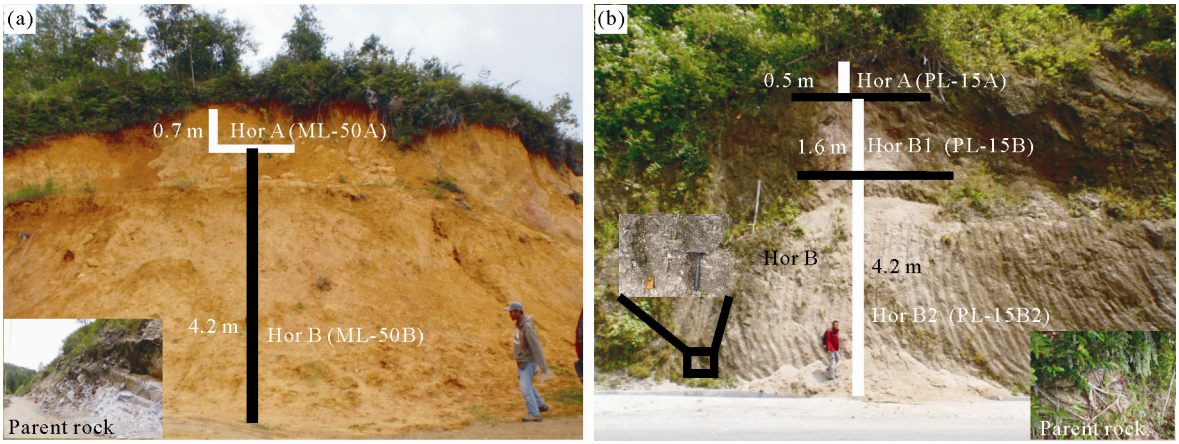

Figure 2. Profile of weathered crust in (a) Mamasa and (b) Palu granitic rocks. Note the weathering profile of Palu granite (b), consisting of horizon A, B1 and B2 whereas Mamasa profile only consists of horizon A and horizon B.

polysynthetic twinning and oscillatory zoning. Alkali-feldspar occurs as microcline, showing characteristic cross-hatched twinning which account for less than 10% of the rocks, sometimes formed mymerkitic texture. Biotite and hornblende are always present in all samples with relatively more biotite than hornblende. Kink band in biotite is commonly observed. Titanite, apatite, zircon and opaque (ilmenite and hematite) mineral served as accessory mineral. Based on the SiO_2 and K_2O content the granitic rocks are mainly classified as calc-alkaline to high calc-alkaline (CAK) series. ASI values range from 0.94 to 1 suggesting that the I-type granitic rocks (Maulana et al., 2011).

Age data on granodiorite in Palu area using K-Ar method yielded 31 Ma (Sukamto, 1996). Similar results were reported on granitoid near Palu area ranging from 31 to 29 Ma (Priadi et al., 1994) and 33.4±0.2 Ma (Elburg et al., 2003). However, a largely younger age on granitic intrusion was reported near Palu-Koro fault, Gimpu and Kulawi region (5.08±0.11 Ma) northern part of Palu (Polvé et al., 1997).

The weathered crusts in Palu granites are relatively thicker and well-developed than those in Mamasa area. They range from 3 to more than 6 meters and can be divided into two (2) horizons; horizon A and B (Fig. 2b). The horizon A (lateritic profile) occur in the upper part of the profile, 0.5 m in thickness, very loose, heavily oxidized, dark brown and contain abundant organic material. Horizon B (weathered horizon) is underlain the horizon A, and can be further divided into B1 and B2 sub horizon in term of their color. The B1 horizon shows relatively dark brown color whereas the B2 horizon is lighter brown to yellowish. Horizon B1 contains lesser amount of organic material but abundant clay mineral whereas horizon B2 show more compact texture and contain clay mineral with quartz is still commonly found. In addition, original texture of the parent rocks is still visible (Fig. 2b).

4 ANALYTICAL METHOD

Twenty two (22) samples were taken from the outcrops of weathered crusts and fresh rock in Mamasa and Palu regions. The major and trace elements composition of the weathered crust and the parent rocks for Mamasa and Palu area are listed in Tables 1 and 2, respectively.

The approximately 1 kg samples were crushed and pulverized to 200 meshes and then thoroughly mixed using a swing mill. Major element compositions were determined on fused disc and pressed powder using an X-ray fluorescence spectrometer Rigaku RINT-300 at Dept. of Earth Resource Engineering, Kyushu University. Rare earth elements (REE) and additional trace elements were analyzed by inductively coupled plasma-mass spectrometry (ICP-MS) in samples previously dissolved with four acid leach (HNO_3-$HClO_4$-HF-HCl) at ALS Chemex laboratory, Vancouver, Canada. Analytical precisions are 1 to 3 percent for major element and better than 5% to 10% for trace and rare earth elements. XRD analysis was conducted in order to determine the mineral composition and clay mineral in the weathered sample. Samples were prepared for XRD analyses by disaggregated in distilled water and the <2 μm fraction was mounted on glass slide and then analyzed using a RIGAKU FKOD 10-015 X-ray diffractometer (XRD) in Dept. of Earth Resources Engineering, Kyushu University.

5 RESULTS

5.1 XRD identification of minerals

Representative powder X-ray diffraction patterns (Cu Kα radiation) are shown in Figs. 3 and 4. Weathered crust of granitic rocks from Mamasa region composed mainly of quartz, kaolinite and montmorrilonite. Quartz was found in all horizons while kaolinite is mainly concentrated in horizon B, showing sharp peaks near 12.2° (7.27 Å) and 19.9° (4.45Å). Montmorillonite was detected in sample ML-43.

Weathered crust at Palu region consists of kaolinite, quartz, albite and halloysite. It is also characterized by the occurrence of quartz in all horizons. Kaolinite was detected in all horizons except in B2 (Fig. 4) whereas halloysite are found in horizon B. Quartz and albite were detected in horizon B2. The occurrences of these rocks forming minerals explain the high content of most major oxide and low content of LOI in the whole rocks composition (Table 2).

5.2 Geochemistry of Weathered and Fresh Granitic Rocks

Concentration of major elements, trace elements and REE of weathered crust and weathering profile from granitic rocks at Mamasa and Palu regions are shown in Tables 1 and 2, respectively and in Fig. 5. Variation of major oxide, trace element and

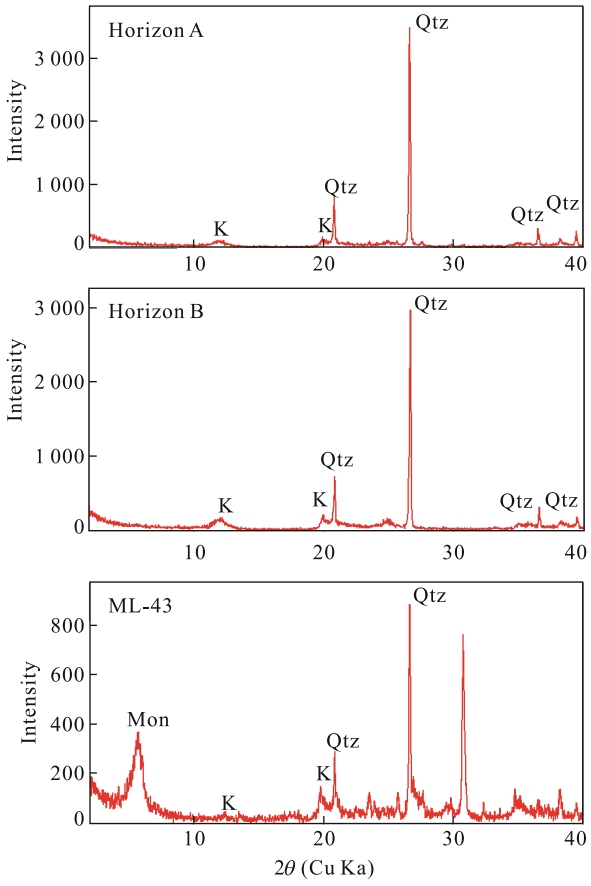

Figure 3. Representative X-ray diffraction pattern of weathered crusts of Mamasa granites. K. Kaolinite; Qtz. quartz; Mon. montmorillonite.

Table 1 Concentration of major elements, trace elements, REE and Y of parent rocks and weathered crust from granitic rocks at Mamasa region

Sample	ML-35	ML-38	ML-41	ML-43	ML-44	ML-46	ML-49	ML-52	ML-50B	ML-50A	Parent rock
Major element (wt.%)									Horizon B	Horizon A	Parent rock
SiO_2	62.0	65.7	57.7	51.1	56.1	55.2	57.4	60.4	55.7	59.2	65.1
TiO_2	0.67	0.34	0.71	0.6	0.85	0.73	0.76	0.73	0.51	0.43	0.62
Al_2O_3	15.3	14.3	15.7	14.6	19.0	19.9	18.1	18.5	25.1	22.4	13.2
FeOt	4.5	2.1	5.1	3.7	5.5	5.3	3.9	4.8	4.5	3.9	4.2
MnO	0.07	0.07	0.09	0.08	0.03	0.05	0.02	0.04	0.03	0.03	0.07
MgO	1.3	1.9	2.9	5.3	1.7	2.7	1.8	2.6	0.9	1.2	4.5
CaO	0.72	0.71	2.93	7.92	1.01	0.05	0.09	0.05	0.02	0.02	3.3
Na_2O	0.86	1.48	1.43	0.46	0.36	0.07	0.21	0.32	0.04	0.06	2.7
K_2O	4.7	5.3	3.9	3.0	3.5	3.1	4.0	4.4	0.03	1.2	4.7
P_2O_5	0.08	0.05	0.34	0.17	0.03	0.02	0.03	0.03	0.03	0.04	0.19
LOI	7.9	7.5	9.1	11.9	9.0	10.8	9.7	5.4	12.1	9.6	0.66
Total	98.2	99.3	99.8	98.8	97.0	97.9	96.0	97.3	99.0	98.2	99.3
Trace element (ppm)											
Co	11.5	8.1	14.3	7.1	10.2	32.9	9.6	24.9	5.1	3.7	17.2
Cr	30	20	40	40	180	280	140	210	50.0	70.0	240.0
Cs	13.5	10.2	10.3	10.1	6.3	20.0	8.5	19.3	15.0	1.9	13.7
Ga	18.4	17	18.9	14.4	24.8	23.4	19.3	22.8	21.8	22.8	20.8
Hf	9	7.3	4.5	5.4	7.5	8.3	12	9.5	5.7	5.4	7.8
Mo	2	<2	<2	6	<2	<2	<2	<2	<2	<2	2.0
Nb	21.9	24.6	18.9	15.7	26.1	23.6	20.2	21.6	13.0	14.6	15.5
Rb	249	283	203	147.5	128.5	132	194	279	75.1	2.6	236.0
Sn	4	5	4	4	13	16	6	8	5.0	6.0	6.0
Sr	207	194.5	301	237	41	56	74.1	88.4	9.9	2.1	223.0
Ta	1.6	1.9	1.5	1.4	1.8	1.8	1.5	1.8	0.9	1.0	1.7
Th	41.7	44.4	36.8	39.9	29.3	29.9	30.5	31.7	13.1	15.7	33.5
Tl	1.3	1.2	0.8	0.7	0.7	0.7	0.8	0.9	<0.5	<0.5	0.9
U	9.9	10.4	6.4	6.3	3.9	6.8	5.6	6.8	2.8	4.2	7.6
V	127	53	127	73	83	86	71	65	57.0	61.0	76.0
W	10	9	6	18	3	5	4	3	5.0	3.0	3.0
Zr	357	255	161	186	292	311	444	343	215.0	204.0	239.0
La	84.7	66.4	72.4	53.2	50.4	110.5	58	103.5	88.6	8.5	52.5
Ce	147	106	129	115.5	133.5	165.5	128	97.2	149.0	25.6	115.0
Pr	13.9	13.5	13.9	11.0	10.8	22.9	12.25	23.1	19.1	2.1	13.1
Nd	47.3	47.7	49.7	36.9	40.0	84.7	45.5	85.7	70.6	8.2	37.6
Sm	7.3	8.1	8.6	6.4	7.0	16.6	7.4	16.8	14.5	2.0	8.1

Continued

Sample	ML-35	ML-38	ML-41	ML-43	ML-44	ML-46	ML-49	ML-52	ML-50B	ML-50A	Parent rock
Trace element (ppm)									Horizon B	Horizon A	Parent rock
Eu	1.4	1.3	1.6	0.9	1.0	2.8	1.0	2.5	2.1	0.1	1.1
Gd	3.9	5.0	5.3	3.7	4.4	12.3	3.8	13.5	12.2	2.1	5.9
Tb	0.78	0.86	0.94	0.57	0.81	2.3	0.7	2.3	2.4	0.5	1.1
Dy	4.8	5.1	5.8	3.0	5.0	14.6	4.1	14.4	16.4	3.6	5.8
Ho	0.93	0.98	1.12	0.52	0.99	2.83	0.78	2.8	3.3	0.8	1.2
Er	2.8	2.8	3.2	1.3	2.9	8.2	2.3	7.9	9.9	2.8	3.0
Tm	0.39	0.39	0.45	0.22	0.4	1.09	0.31	1.08	1.4	0.4	0.6
Yb	2.6	2.6	2.8	1.4	2.5	6.6	2.0	6.6	8.1	2.8	3.0
Lu	0.42	0.41	0.45	0.2	0.4	0.98	0.32	0.95	1.2	0.4	0.5
Y	28.1	29.2	32.7	14.8	27.5	80.7	24.5	76.4	94.4	23.2	37.0
LREE	301.6	243.0	275.2	223.8	242.7	403.0	252.2	328.8	343.8	46.5	227.4
HREE	16.7	18.1	20.1	10.9	17.5	48.8	14.3	49.5	54.9	13.4	21.0
Total REE	318.3	261.1	295.3	234.7	260.2	451.8	266.5	378.2	398.7	59.9	248.4
REE+Y	346.4	290.3	328.0	249.5	287.7	532.5	291.0	454.6	493.1	83.1	285.4
Ce/REE	0.46	0.41	0.44	0.49	0.51	0.37	0.48	0.26	0.37	0.43	0.46
(La/Yb)N	32.2	25.2	25.6	39.1	19.9	16.7	29.0	15.7	7.8	2.1	12.4
Ce/La	1.7	1.6	1.8	2.2	2.6	1.5	2.2	0.94	1.7	3.0	2.2
Eu/Sm	0.19	0.16	0.19	0.14	0.14	0.17	0.14	0.15	0.14	0.06	0.14

Table 2 Concentration of major elements, trace elements, REE and Y of parent rocks and weathered crust from granitic rocks at Palu region

Sample	PL-13	PL-14	PL-15B3	PL-15C1	PL-17	PL-19A	PL-21B	PL-15B2	PL-15B	PL-15A	Parent rock
Major element (wt.%)								Hor-B2	Hor-B1	Hor-A	Parent rock
SiO_2	57.9	56.8	52.9	63.6	65.0	67.8	65.5	65.2	53.3	55.5	66.1
TiO_2	0.67	0.54	0.86	0.59	0.69	0.56	0.74	0.67	1.6	0.74	0.49
Al_2O_3	14.3	15.7	19.3	15.3	14.6	14.3	13.3	14.2	23.0	20.0	14.3
FeOt	4.0	6.9	7.5	4.8	4.8	3.2	4.1	4.1	9.5	6.2	3.6
MnO	0.06	0.06	0.07	0.05	0.1	0.03	0.09	0.09	0.08	0.06	0.05
MgO	2.8	1.7	3.0	2.5	2.7	1.6	3.4	3.2	2.5	2.8	2.7
CaO	2.8	1.6	0.67	0.99	3.7	0.11	3.5	4.0	0.25	0.47	3.2
Na_2O	1.8	2.2	0.4	0.73	2.1	1.5	3.1	2.5	0.23	0.34	3.4
K_2O	4.7	3.5	2.7	2.2	4.0	4.3	4.4	3.5	1.0	2.2	4.0
P_2O_5	0.34	0.21	0.16	0.08	0.23	0.11	0.41	0.30	0.11	0.09	0.27
H_2O	3.2	8.6	6.7	7.9	1.8	3.3	1.1	2.2	8.2	9.5	1.1
Total	92.6	97.7	94.2	98.8	99.7	96.8	99.6	99.9	99.9	98.0	99.1
Trace element (ppm)											
Co	11.2	8.3	10.3	13	12.1	7.8	13.7	12.7	21.2	13.4	10.7
Cr	80	69.3	120	80	60	60	110	90.0	20.0	90.0	80.0
Cs	11.5	10.8	3.45	3.77	5.16	6.51	1.96	18.85	8.94	4.06	5.26
Ga	19.4	22.0	18.3	16.3	20.8	17.6	18	20.1	24.3	19.8	18.9
Hf	5.8	4.7	5	4	4.5	5.6	3.8	5.5	6.8	4.2	6.5
Mo	<2	<2	<2	<2	<2	<2	<2	<2	<2	<2	<2
Nb	18.6	17.4	9.5	8.4	14.3	16.8	11.4	22.5	10.9	8.4	16.1
Rb	280	278.3	99.1	96.2	182.5	207	153	250.0	58.1	103.5	186.0
Sn	5	4.0	2	1	3	3	2	6.0	2.0	1.0	4.0
Sr	587	468.2	157	127.5	435	228	758	515.0	29.8	73.1	747.0
Ta	1.8	1.9	0.7	0.5	1.1	1	0.6	2.3	0.70	0.60	1.7
Th	29.6	34.5	12.8	9.8	24.5	20.1	9	50.6	4.6	11.1	35.3
Tl	1.4	2.7	<0.5	<0.5	0.8	1	0.7	1.2	<0.5	<0.5	1.1
U	14.5	18.6	2.6	1.8	4.5	4.9	2.3	11.5	1.1	1.9	10.3
V	124	102.3	166	126	106	83	105	97.0	166.0	152.0	88.0
W	2.0	2.0	10.0	2.0	2.0	3.0	2.0	2.0	2.0	2.0	1.0
Zr	219	186.5	176	153	144	234	146	186.0	279.0	160.0	213.0
La	61.6	55.7	32.1	27.9	48.8	40.3	45.8	80.0	28.2	23.8	43.6
Ce	114.5	106.3	69.4	58.2	90.3	75.3	93.4	145.5	61.3	53.5	89.2
Pr	12.0	9.3	7.9	6.31	9.47	8.02	10.85	14.8	9.2	6.0	9.8
Nd	41.3	38.9	28.9	24.4	33.7	28.3	40.9	51.1	43.0	22.6	26.8
Sm	6.6	6.7	6.22	4.76	5.69	4.98	7.45	7.8	10.6	4.6	5.1

Continued

Sample	PL-13	PL-14	PL-15B3	PL-15C1	PL-17	PL-19A	PL-21B	PL-15B2	PL-15B	PL-15A	Parent rock
Trace element (ppm)								Hor-B2	Hor-B1	Hor-A	Parent rock
Eu	1.3	1.2	1.33	0.96	1.17	0.99	1.57	1.4	2.8	0.8	1.2
Gd	3.3	4.2	5.19	4.16	3.22	2.95	4.64	3.5	9.9	3.5	3.2
Tb	0.64	0.66	0.89	0.78	0.60	0.56	0.8	0.67	1.58	0.60	0.53
Dy	3.65	3.85	5.31	5.1	3.42	3.42	4.92	4.11	10.15	3.54	2.74
Ho	0.68	0.58	1.03	1.09	0.68	0.69	0.94	0.75	2.0	0.69	0.53
Er	1.89	1.8	2.9	3.25	2	2.09	2.72	2.1	6.0	2.0	1.4
Tm	0.27	0.22	0.48	0.46	0.28	0.29	0.36	0.30	0.82	0.31	0.25
Yb	1.83	2.0	2.8	2.81	1.68	2.04	2.3	1.9	5.1	1.9	1.5
Lu	0.27	0.36	0.46	0.45	0.28	0.33	0.34	0.30	0.80	0.31	0.24
Y	20	19.8	27.2	29	19.7	20.1	26.8	23.0	57.8	20.4	18.3
LREE	237.3	218.1	145.9	122.5	189.1	157.9	200.0	300.6	155.1	111.3	175.7
HREE	12.5	13.6	19.1	18.1	12.2	12.4	17.0	13.7	36.4	12.8	10.3
E REE	249.8	231.7	164.9	140.6	201.3	170.3	217.0	314.3	191.5	124.1	186.0
REE+Y	269.8	251.5	192.1	169.6	221.0	190.4	243.8	337.3	249.3	144.5	204.3
Ce/REE	0.46	0.46	0.42	0.41	0.45	0.44	0.43	0.46	0.32	0.43	0.48
La/Yb	33.7	28.4	11.5	9.9	29.0	19.8	19.9	30.0	4.0	8.8	7.1
Ce/La	1.9	1.9	2.2	2.1	1.9	1.9	2.0	1.8	2.2	2.2	2.0
Eu/Sm	0.20	0.18	0.21	0.20	0.21	0.20	0.21	0.17	0.26	0.18	0.22

REE in the weathered crusts from the granitic rocks are summarized in Fig. 6.

5.2.1 Major element

The parent rock in Mamasa profile contains of 65 wt.% SiO_2, 13 wt.% of Al_2O_3, 2.6 wt.% Na_2O, 4.7 wt.% K_2O, 3.3 wt.% CaO and less than 1 wt.% TiO_2 and P_2O_5. In relation to this, the weathering profile show high content of Al_2O_3 and LOI, and lower content of other oxides. The FeO total content in horizon B however shows higher content than the parent rock. The chemical differences are pronounced for the weathering profile where the K-feldspar, plagioclace, biotite and hornblende are transformed into kaolinite and hematite.

Overall, most major elements (particularly SiO_2) from Palu weathering profile are significantly depleted to their parent granites. In contrast, Al_2O_3, FeO total and LOI are significantly increased. TiO_2 and P_2O_5 tend to immobile during weathering process. An exception is showed in the horizon B-2 in which the SiO_2, MgO, FeO total and CaO content increase and steadily decreased toward the horizon A.

5.2.2 Trace and rare earth element

As compared to their parent granites, content of Th and U are lower whereas Zr and Hf are relatively constant in Mamasa profiles but increase in Palu profile. These representing that the weathering resistant mineral (zircon) is strongly concentrated in both weathering profile. Trace elements such as Rb and Sr relatively decreased (except in the horizon B2 in Palu profile) toward the upper profile whereas Sn, W and Ta show relatively no significant variation.

The concentrations of the rare earth elements are vary in each horizon (Fig. 5). The total REE contents of the weathered crusts at the Mamasa region range from 58 ppm to 398 ppm whereas those of fresh (parent) rocks are 248 ppm. The total LREE content of the weathered samples ranges from 46 ppm to 343 ppm whereas the total of HREE content ranges from 13 ppm to 54 ppm.

The total REE in the weathered crusts at Palu region ranges from 124 ppm to 314 ppm (223 ppm in average) whereas the total REE in the parent rock range from 196 ppm to 251 ppm (200 ppm in average). The total REE+ Y in the weathered crust ranges from 220 ppm to 337 ppm and 198 ppm to 267 ppm in the parent rocks. The enrichment of REE occurred mainly in the horizon B2, where the total REE is up to 314 ppm (REE+Y=337 ppm). It is shown that the REE are significantly depleted in the horizon A in both profiles but showed approximately 70% to 85% larger than the parent rocks in horizon B. This result indicated that the enrichment of REE occurred in horizon B in both profiles.

6 DISCUSSION

6.1 Distribution of REE in the Weathering Profile

$(La/Yb)_N$ and Eu/Sm decreased toward the upper part of the Mamasa profile whereas Ce/total REE is relatively constant

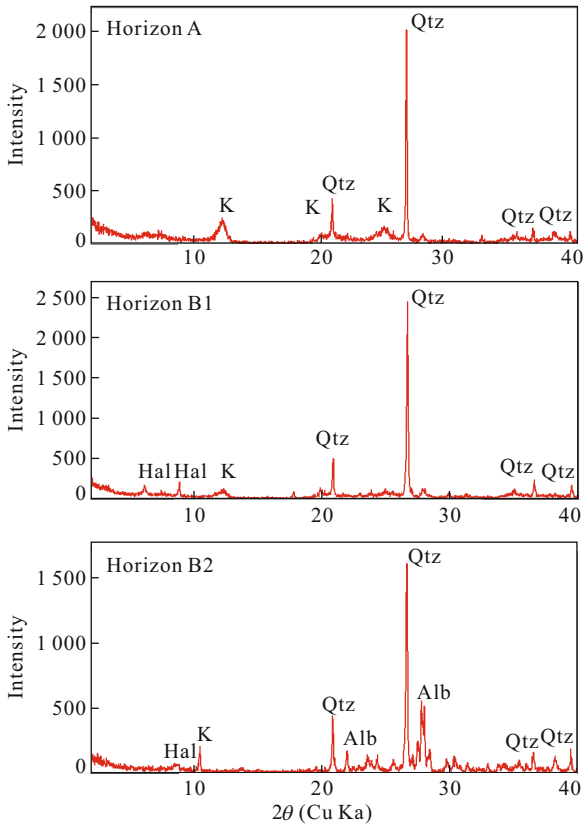

Figure 4. Representative X-ray diffraction pattern of weathered crusts of Palu granites. K. Kaolinite; Qtz. quartz; Alb. albite; Hal. halloysite.

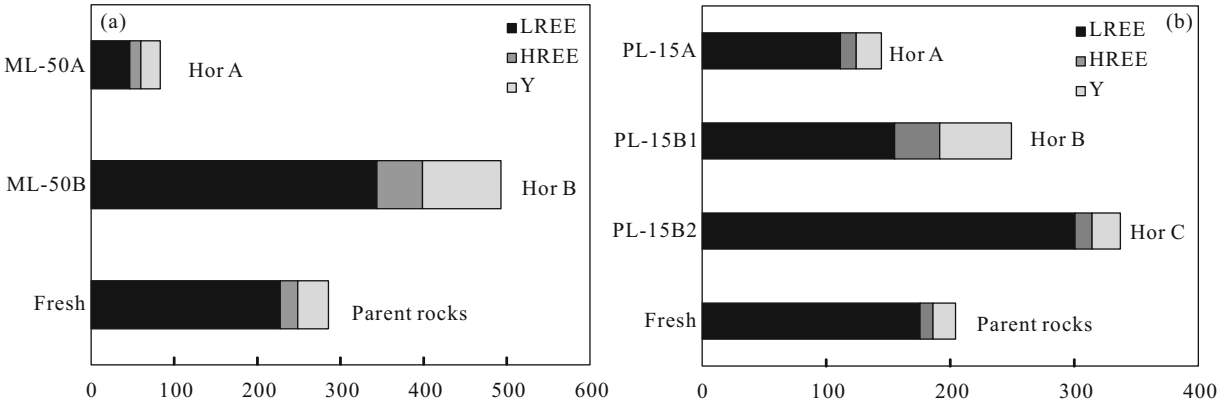

Figure 5. Total LREE, HREE and Y of weathered crusts at (a) Mamasa and (b) Palu.

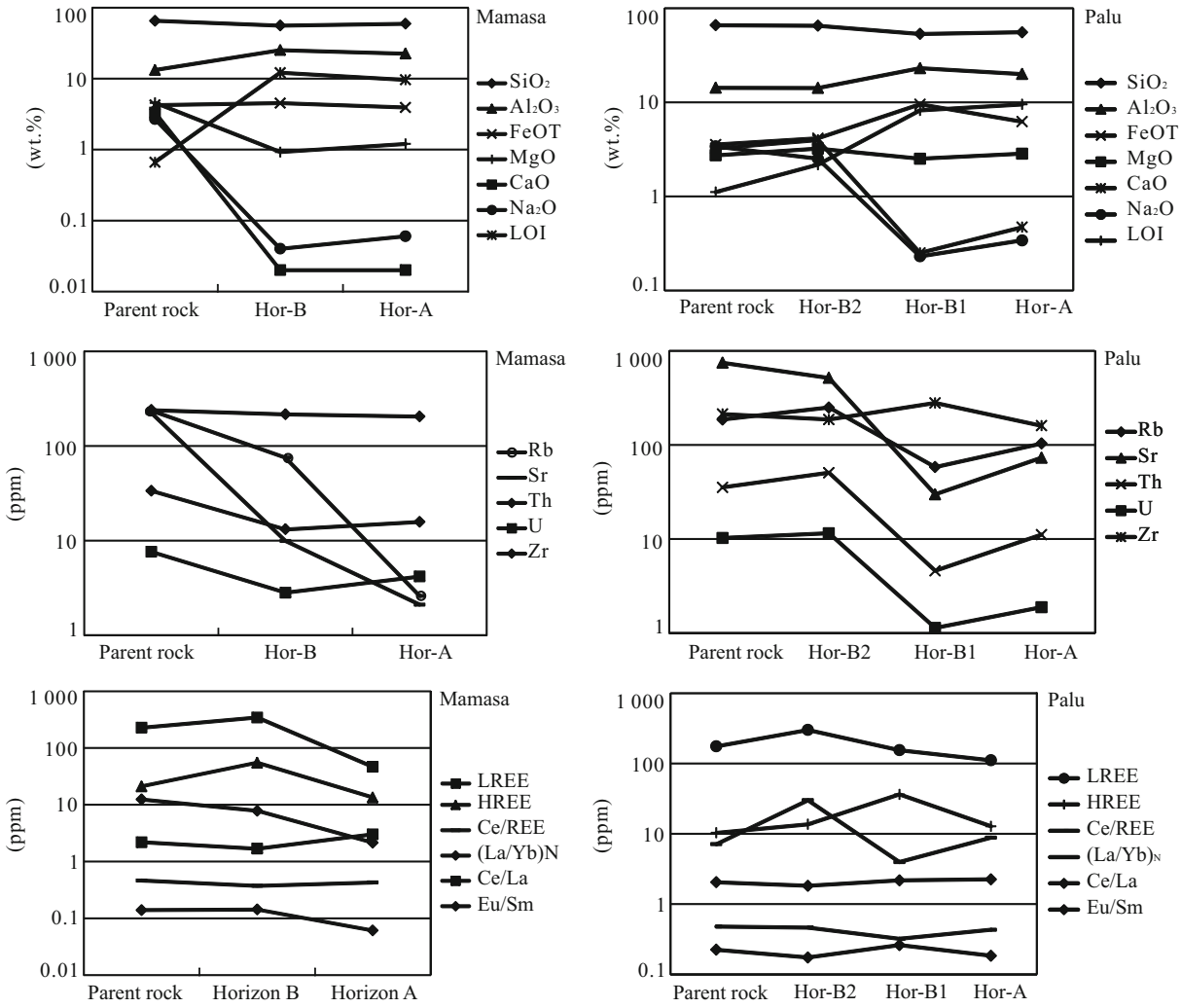

Figure 6. Variation in major element oxide, trace element and REE in Mamasa and Palu weathering profile.

and Ce/La show insignificant changes vertically. The LREE and HREE increased from the parent rock to the horizon B but decreases significantly to the horizon A suggests that there were prominent enrichment of REE in the horizon B.

The weathered profile at Palu also show a vertical variation in which total LREE increased from the parent rocks to the horizon B2 but decreased toward the horizon B1 and finally increased in the horizon A. The enrichment of LREE in the horizon B2 is also supported by the increasing trend of $(La/Yb)_N$ value from the parent rocks toward the horizon B2 but drastically depleted toward the horizon B1 and A as (Table 2). This suggests that a prominent enrichment of LREE are occurred the horizon B2. It is interesting to note that the HREE are significantly increased in B1 profile (Fig. 6), indicating that the HREE are enriched toward the horizon B1 but significantly decreased in horizon A. Ce/La, Ce/total REE and Eu/Sm are steadily constant toward the upper part of the profile but the values are relatively higher than those of the Mamasa profile.

Chondrite-normalized (Sun and McDonough, 1989) REE pattern (Fig. 7) of the weathered crust are relatively higher to their parent rocks in both profiles. The total REE content of the weathered crust are relatively elevated compared to the parent rocks. These suggest that REE-bearing accessory minerals may be resistant against weathering and may remain as residual phase in the weathered crusts, particularly in the lower part of horizon B in Mamasa profile and in horizon B2 in Palu profile. The occurrences zircon, apatite and allanite as major REE-bearing accessory minerals have been reported in the parent rocks in both areas (Maulana et al., 2011). The relatively similar Zr concentration between the parent rocks and the weathered crust also support this idea. It is interesting to note that the horizon B1 in Palu profile show relatively higher HREE content compare to other horizons. The enrichment of HREE is concordant with the high Zr content indicating the zircon role. Alternatively, the higher content of HREE in this horizon may be due to the abundance of clay mineral (e.g., kaolinite and halloysite). However, the relationship between the clay minerals and HREE enrichment should be verified by extraction test in order to determine the ion adsorption process.

Both weathered and fresh granitic rocks from the study area show significant negative Eu anomaly (Eu/Eu*< 1), indicating plagioclase fractionation during magmatism. These anomalies appear to be inherited from their parent rocks.

6.2 Mass Transfer during Weathering Process

In order to evaluate mass transfer during weathering pro-

cess in the granitic rocks in both regions, we applied isocon method calculation as suggested by Grant (1986). The normalization solution method was taken from Guo et al. (2009) and the results are expressed in isocon diagram (Fig. 8). The scaling used in these diagrams are the same as those employed by Guo et al. (2009) and Grant (1986) with some modification particularly for REE.

In the normalized isocon diagram, the mass changes of any components in each horizon within the weathering profile can be evaluated by reading the corresponding data points. The Mamasa isocon diagram shows that from the B horizon to the A horizon Al_2O_3, FeOT, MgO, K_2O and SiO2 were gained whereas CaO and Na_2O were relatively immobile and LREE, HREE and total REE were lost. The trend of mass transfer shows a trend of initial gain of LREE, HREE and total REE in horizon B which was followed by a progressive losses trend toward horizon A. The Palu isocon shows a slightly different trend. For example, from the horizon B2 to the horizon A , LOI, FeOT and Al_2O_3 were gained, whereas other oxides, LREE, HREE and total REE were lost. K_2O, CaO, Na_2O, LREE and total REE underwent an initial gain in the horizon B2 but then progressively lost toward the upper part of the profile. Meanwhile, after having been gained in the horizon B1 from the parent rock, HREE were progressively lost to the horizon A.

6.3 Ce Anomaly

During chemical weathering, cerium (Ce) tends to behave differently from other REE (Bao and Zhao, 2008; Henderson, 1984). Cerium in oxidizing environment occurs as Ce^{4+}, highly insoluble as CeO_2 whereas the other REE maintain their 3+ ionic states and are leached by circulating water (Marsh, 1991). Positive anomaly of Ce(Ce/Ce*) occur in the horizon A in weathering profile of granitic rocks (e.g., South China and Laos).

Ce anomaly of the samples in Mamasa and Palu areas is ranging from 1.6 to 5.7, except that from the horizon B in Mamasa profile (Ce/Ce*=6). The weathered crusts from the horizon A in Mamasa profile has positive Ce anomaly whereas the horizon B show a negative anomaly (Fig. 7). The positive anomaly of Ce in the weathered crust suggests that Ce is fixed as Ce (IV) due to oxidation in the aqueous phase after being dissolved initially as Ce (III). The positive Ce anomaly in the

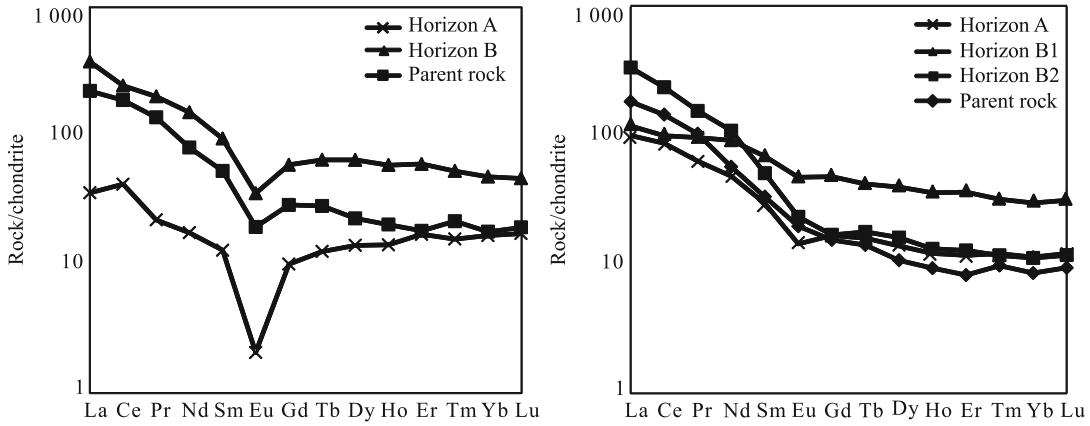

Figure 7. Chondrite normalized rare earth element pattern of parent rocks and weathered granitic rocks from Mamasa and Palu.

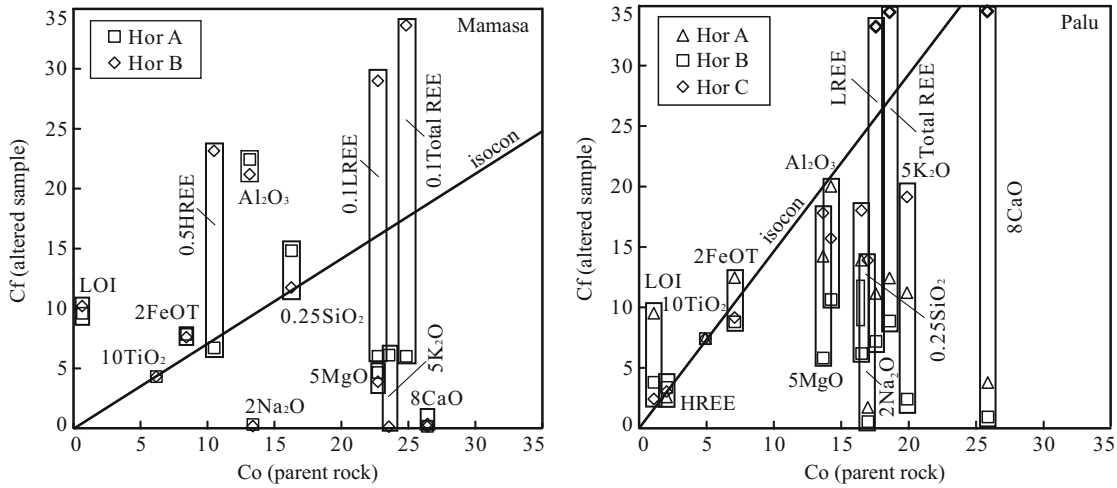

Figure 8. Normalized isocon diagrams for the weathering profile in the granitic rocks from Mamasa and Palu regions using the normalization solution. The thick line indicates the unified isocon defined by TiO_2 and the number before the oxide and REE symbol represent the scaling coefficients.

horizon A indicated that Ce is rapidly precipitated during weathering and retain at the upper soil horizon.

7 CONCLUSIONS

The weathered crusts in Palu are relatively thicker and well-developed than in Mamasa region. In both areas, the enrichment of REE is mainly occurred in the horizon B (Mamasa) and B2 (Palu). The weathered crusts in Mamasa and Palu regions show relatively higher concentration of total REE and REE+Y compared to their parent rocks.

XRD result shows that the weathered crust from Mamasa and Palu granitic rocks composed mainly of quartz, plagioclase, kaolinite, montmorillonite and halloysite.

The enrichments of REE in the horizon B in both profiles suggest that the REE enrichment is controlled by the weathering resistance of the principal REE-bearing accessory mineral in the parent rocks which remain as residual phase in the weathered crusts.

The mass transfer illustration using isocon diagram shows a different transfer trend from Mamasa and Palu weathering profile.

The positive Ce anomaly in the horizon A indicated that Ce is rapidly precipitated during weathering and retain at the upper soil horizon.

ACKNOWLEDGMENTS

The first author is thankful to the Ministry of Education and Sport (MEXT) for PhD scholarship. Financial support assistance from Global-Centre of Excellent (GCOE) program Kyushu University is also highly acknowledged.

REFERENCES CITED

Alderton, D. H. M., Pearce, J. A., Potts, P. J., 1980. Rare Earth Element Mobility during Granite Alteration: Evidence from Southwest England. *Earth and Planetary Science Letters*, 49(1): 149–165

Bao, Z. W., Zhao, Z. H., 2008. Geochemistry of Mineralization with Exchangeable REY in the Weathering Crusts of Granitic Rocks in South China. *Ore Geology Review*, 33: 519–535

Bergman, S. C., Coffield, D. Q., Talbot, J. P., et al., 1996. Tertiary Tectonic and Magmatic Evolution of Western Sulawesi and the Makassar Strait, Indonesia: Evidence for a Miocene Continent-Continent Collision. In: Hall, R., Blundell, D., eds., Tectonic Evolution of Southeast Asia. *Geological Society*, *London*, *Special Publications*, 106: 391–429

Braun, J., Pagel, M., Muller, J., et al., 1990. Cerium Anomalies in Lateritic Profiles. *Geochimica et Cosmochimica Acta*, 54(3): 781–795

Condie, K. C., Baragar, W. R. A., 1974. Rare Earth Element Distribution in Volcanic Rocks from Archean Greenstone Belts. *Contributions to Mineralogy and Petrology*, 45(3): 237–246

Djuri, S., 1998. Geology of Majene Quadrangle, 1 : 250 000 in Scale. Geology Research and Development Centre, Bandung

Elburg, M., Foden, J., 1999. Sources for Magmatism in Central Sulawesi: Geochemical and Sr-Nd-Pb Constraints. *Chemical Geology*, 156: 67–93

Elburg, M. A., van Leeuwen, T., Foden, J., et al., 2003. Spatial and Temporal Isotopic Domains of Contrasting Igneous Suites in Western and Northern Sulawesi, Indonesia. *Chemical Geology*, 199: 243–276

Gouveia, M. A., Prudêncio, M. I., Figueiredo, M. O., et al., 1993. Behavior of REE and other Trace and Major Elements during Weathering of Granitic Rocks, Évora, Portugal. *Chemical Geology*, 107(3–4): 293–296

Grant, J. A., 1986. The Isocon Diagram—A Simple Solution to Gresens Equation for Metasomatic Alteration. *Economic Geology*, 81: 1976–1982

Guo, S., Ye, K., Chen, Y., et al., 2009. A Normalization Solution to Mass Transfer Illustration of Multiple Progressively Altered Samples Using the Isocon Diagram. *Economic Geology*, 104: 881–886

Hamilton, W. B., 1979. Tectonics of the Indonesian Region. Geological Survey Professional Paper 1078. USGS, Washington. 345

Henderson, P., 1984. Rare Earth Element Geochemistry. Elsevier, Amsterdam. 510

Hu, Z., Gao, S., 2008. Upper Crustal Abundances of Trace Elements: A Revision and Update. *Chemical Geology*, 253: 205–221

Ishihara, S., Hua, R., Hoshino, M., et al., 2008. REE Abundance and REE Minerals in Granitic Rocks in the Nanling Range, Jiangxi Province, Southern China, and Generation of the REE-Rich Weathered Crusts Deposits. *Resource Geology*, 58(4): 355–372

Marsh, J. S., 1991. REE Fractionation and Ce Anomalies in Weathered Karoo Dolerite. *Chemical Geology*, 190: 189–194

Maulana, A., Watanabe, K., Imai, A., et al., 2011. Geochemical Variation of Granitic Rocks in Sulawesi Island, Indonesia. *Proceeding of International Symposium on Earth Science and Technology 2011*, 379–387

Nesbitt, H. W., Young, G. M., 1984. Prediction of Some Weathering Trends of Plutonic and Volcanic Rocks Based on Thermodynamic and Kinetic Considerations. *Geochemica et Cosmochimica Acta*, 48: 1523–1534 (not cited)

Parkinson, S., 1998. An Outline of the Petrology, Structure and Age of the Pompangeo Schist Complex of Central Sulawesi, Indonesia. *Island Arc*, 7: 231–245

Pearce, J. A., Cann, J. R., 1973. Tectonic Setting of Basic Volcanic Rocks Determined Using Trace Element Analyses. *Earth and Planetary Science Letters*, 19: 290–300

Polvé, M., Maury, R. C., Bellon, H., et al., 1997. Magmatic Evolution of Sulawesi (Indonesia): Constraints on the Cenozoic Geodynamic History of the Sundaland Active Margin. *Tectonophysics*, 272: 69–92

Priadi, B., Polvé, M., Maury, R. C., et al., 1994. Tertiary and Quaternary Magmatism in Central Sulawesi: Chronological and Petrological Constraints. *Journal of Southeast Asian Earth Science*, 9: 81–93

Priadi, B., Sucipta, I. G. B. E., Utoyo, H., et al., 1996.

Kompleks Granitoid Neogen Di Sulawesi Tengah, Tinjauan Geokimia. *Bulletin Geology* (*in Indonesia*), 26: 129–141

Sanematsu, K., Murakami, H., Watanabe, Y., et al., 2009. Enrichment of Rare Earth Element in Granitic Rocks and their Weathered Crusts in Central and Southern Laos. *Bulletin of the Geological Survey of Japan*, 60 (11–12): 527–558

Sanematsu, K., Kon, Y., Imai, A., et al., 2011. Geochemical and Mineralogical Characteristic of Ion-Adsorption Type REE Mineralization in Phuket, Thailand. *Mineralium Deposita*, 48(4): 437–451, doi:10.1007/s00126-011-0380-5

Sukamto, R., 1996. Reconnaissance Geological Map of the Palu Quadrangle, Sulawesi. 1–250 000 in Scale. Geological Research and Development Centre, Bandung

Sukamto, R., 1975. Geological Map of Indonesia, Ujung Pandang Sheet-Scale 1 : 1 000 000. Geological Survey of Indonesia, Bandung

Sun, S. S., McDonough, W. F., 1989. Chemical and Isotopic Systematics of Oceanic Basalts: Implications for Mantle Composition and Processes. In: Saunders, A. D., Norry, M. J., eds., Magmatism in Ocean Basins. *Geological Society London*, *Special Publication*, 42: 313–345

Van Leeuwen, T., Allen, C. M., Kadarusman, A., et al., 2007. Petrologic, Isotopic and Radiometric Age Dating Constraints on the Origin and Tectonic History of the Malino Metamorphic Complex, NW Sulawesi, Indonesia. *Journal of Asian Earth Sciences*, 29: 751–777

Winchester, J. A., Floyd, P. A., 1976. Geochemical Magma Type Discrimination: Application to Altered and Metamorphosed Basic Igneous Rocks. *Earth and Planetary Science Letters*, 28: 459–469